Development 129, 3173-3183 (2002)
Printed in Great Britain © The Company of Biologists Limited 2002
DEV5501

Drosophila RhoA regulates the cytoskeleton and cell-cell adhesion in the developing epidermis

James W. Bloor and Daniel P. Kiehart*

Developmental, Cell and Molecular Biology Group, Department of Biology, B330 LSRC Building, Duke University, Durham, NC 27708-1000, USA
*Author for correspondence (e-mail: dkiehart@duke.edu)

Accepted 8 March 2002

SUMMARY

The small GTPase Rho is a molecular switch that is best known for its role in regulating the actomyosin cytoskeleton. We have investigated its role in the developing *Drosophila* embryonic epidermis during the process of dorsal closure. By expressing the dominant negative DRhoA^{N19} construct in stripes of epidermal cells, we confirm that Rho function is required for dorsal closure and demonstrate that it is necessary to maintain the integrity of the ventral epidermis. We show that defects in actin organization, nonmuscle myosin II localization, the regulation of gene transcription, DE-cadherin-based cell-cell adhesion and cell polarity underlie the effects of DRhoA^{N19} expression. Furthermore, we demonstrate that these changes in cell physiology have a differential effect on the epidermis that is dependent upon position in the dorsoventral axis. In the ventral epidermis, cells either lose their adhesiveness and fall out of the epidermis or undergo apoptosis. At the leading edge, cells show altered adhesive properties such that they form ectopic contacts with other DRhoA^{N19}-expressing cells.

Movies available on-line

Key words: *Drosophila*, RhoA GTPase, DE-cadherin, Dorsal closure

INTRODUCTION

During embryonic development and organogenesis, coordinated changes in individual cell shape contribute to the large-scale cell sheet movements that are characteristic of morphogenesis. Many such movements are generated through local contraction of the actin cytoskeleton, driven by the molecular motor protein nonmuscle myosin II. This is clearly demonstrated in *Drosophila* where mutations in *zipper* (*zip*) and *spaghetti squash* (*sqh*), genes that encode nonmuscle myosin II subunits, cause lethality and are associated with defects in cell division (Karess et al., 1991; Ohshiro et al., 2000; Peng et al., 2000), cell polarity (Winter et al., 2001), muscle development (Bloor and Kiehart, 2001), and the morphogenetic processes of leg elongation, head involution and dorsal closure (Cote et al., 1987; Edwards and Kiehart, 1996; Halsell et al., 2000; Nusslein-Volhard et al., 1984; Young et al., 1993; Zhao et al., 1988).

Dorsal closure describes the process by which the developing embryo becomes enclosed by the epidermis and serves as an excellent model for studying morphogenesis. It begins when, on both sides of the embryo, the dorsal-most lateral epidermal cells become organized into a well-defined row that possesses at its dorsal edge a supracellular purse-string of actin and nonmuscle myosin II (Young et al., 1993). These 'leading edge' cells overlie and adhere to the peripheral cells of the amnioserosa, an epithelium that occupies the dorsal surface of the embryo. As dorsal closure proceeds, the leading edge actomyosin purse-string contracts (Kiehart et al., 2000) and, beginning with the leading edge, lateral epidermal cells elongate dorsally. In addition, the amnioserosa contracts and concomitantly a small number of cells drop out of this epithelial layer. As a result, the amnioserosa diminishes in size as dorsal closure proceeds (Kiehart et al., 2000). The overall effect is that, while the amnioserosa ultimately sinks internally where it undergoes apoptosis, the two halves of the lateral epidermis progress towards the dorsal midline. As they approach each other the opposing epithelial sheets suture together, a bidirectional process that appears to be aided by leading edge filopodia (Jacinto et al., 2000).

Genetic analysis of dorsal closure has been a particularly effective tool with which to identify and dissect pathways that regulate morphogenetic movements. For example, mutations in components of the JNK (Jun N-terminal kinase) transcriptional activation pathway (Glise et al., 1995; Hou et al., 1997; Kockel et al., 1997; Martin-Blanco et al., 1998; Riesgo-Escovar et al., 1996; Riesgo-Escovar and Hafen, 1997; Sluss et al., 1996) and the *decapentaplegic* (*dpp*) signaling pathway (Affolter et al., 1994; Arora et al., 1995; Brummel et al., 1994; Grieder et al., 1995; Letsou et al., 1995; Nellen et al., 1994; Penton et al., 1994; Ruberte et al., 1995; Staehling-Hampton et al., 1995) fail to complete dorsal closure, leaving the dorsal surface of the embryo open. Ectopic expression of RhoGTPase family constructs also disrupt dorsal closure (Harden et al., 1995; Harden et al., 1999; Ricos et al., 1999). Thus, expression of dominant-negative Rac^{N17} results in the

formation of a dorsal hole. Rac^{N17} expression, like mutations in the JNK pathway, disrupts formation of the leading edge actomyosin purse-string. Moreover, constitutively active Rac induces ectopic epidermal expression of *dpp* and *puc*, known targets of JNK signaling in the leading edge (Glise and Noselli, 1997). As this induction is dependent on the JNK pathway and as Rac is an activator of JNK signaling in vertebrates (Coso et al., 1995; Minden et al., 1995), this suggests that Rac activates the JNK cascade in the leading edge. Epidermal expression of constitutively active Cdc42 also induces ectopic expression of *dpp* and *puc* (Glise and Noselli, 1997). However, loss of function *Cdc42* mutations have no effect on leading edge dpp expression (Genova et al., 2000). In addition, although expression of dominant-negative Cdc42 disrupts dorsal closure, it does not cause complete disruption of the leading edge actomyosin purse-string (Harden et al., 1999; Ricos et al., 1999; Riesgo-Escovar et al., 1996). Rather, the leading edge defects observed phenocopy those exhibited by mutants for downstream components of the DPP pathway. DPP signaling acts subsequent to JNK activation and is thought to mediate elongation of lateral epidermal cells (Riesgo-Escovar and Hafen, 1997). Thus, while evidence on Cdc42 function in dorsal closure is somewhat ambiguous, the simplest interpretation puts Cdc42 signaling downstream of DPP. This is supported by the ability of constitutively active Cdc42 to partially rescue of mutations in the DPP receptor, *thickveins* (Ricos et al., 1999).

Expression of dominant-negative Rho^{N19} also disrupts dorsal closure. However, it is unclear how Rho fits into the pathway described above. Thus, Rho^{N19} expression results in loss of actin and nonmuscle myosin II from the leading edge, but only in leading edge cells that flank the segment borders (Harden et al., 1999). Alternatively, targeted expression of this Rho construct in the leading edge disrupts elongation of all leading edge cells (Lu and Settleman, 1999). This defect is similar to that seen in JNK pathway mutants, however dominant negative Rho does not disrupt *dpp* expression, suggesting that JNK pathway activation is unaffected. A role for Rho in dorsal closure is also supported by genetic evidence; zygotic mutations in the *RhoA* gene (*Rho1* – FlyBase) result in the puckering of the dorsal midline (Magie et al., 1999). Depletion of maternally contributed Rho leads to severe defects early in development, suggesting that under normal conditions there is sufficient maternal contribution of Rho to affect an aberrant dorsal closure.

Rho is known to activate cellular contractility by modulating phosphorylation of the nonmuscle myosin II regulatory light chain (reviewed by Bresnick, 1999) and interacts genetically with nonmuscle myosin II in *Drosophila* (Halsell and Kiehart, 1998; Winter et al., 2001). As endogenous *RhoA* is ubiquitously expressed during embryogenesis (Hariharan et al., 1995), this suggests that Rho could function in dorsal closure by activating contraction within either the amnioserosa and/or leading edge actomyosin purse-string. Alternatively, in cultured vertebrate epithelial cells, Rho is required for formation and maintenance of E-cadherin mediated cell junctions (Braga et al., 1999; Braga et al., 1997; Zhong et al., 1997), suggesting that Rho may play a more fundamental role in the development of the *Drosophila* epidermis. Thus, a reduction in Rho function could disrupt the integrity of both the amnioserosa and epidermis through effects on the cytoskeleton and/or cell-cell junctions, thereby causing a defect in dorsal closure.

We have focused on the role of *Drosophila* RhoA in epidermal development by expressing the dominant-negative $DRhoA^{N19}$ construct (Strutt et al., 1997) in stripes of epidermal cells. This form of RhoA is thought to remain in an inactive GDP-bound state that binds to and sequesters endogenous guanine nucleotide exchange factors, thereby preventing activation of endogenous Rho. We confirm that striped epidermal expression of $DRhoA^{N19}$ causes dorsal closure to fail and we show that actin and nonmuscle myosin II localization is disrupted in all the leading edge cells that express $RhoA^{N19}$. Surprisingly, we find that rather than blocking the JNK transcriptional activation pathway, the inhibition of RhoA function leads to its ectopic activation in the lateral epidermis. $RhoA^{N19}$ expression also severely affects the integrity of the ventral epidermis. Live imaging shows that ventral epidermal cells lose adhesiveness, frequently fall out of the epithelial cell layer and appear to undergo apoptosis. By contrast, dorsal cells alter their adhesive properties, such that they form ectopic adhesions with cells within adjacent $RhoA^{N19}$-expressing stripes via extensive filopodia. We show that both phenotypes are associated with loss of cell polarity and *Drosophila* E-cadherin from the surface of $RhoA^{N19}$-expressing cells. These observations suggest that RhoA has distinct repertoires of function in different epidermal domains. Within the ventral and lateral epidermis, RhoA is essential for proper actomyosin cytoskeletal organization, is involved in regulating gene transcription and promotes cell-cell adhesion; within the leading edge, RhoA is required for the formation of the leading edge purse-string and acts to restrict inappropriate cell-cell adhesion.

MATERIALS AND METHODS

Drosophila stocks and crosses

The following mutations and transgenes were used in this study: *p[w+,enGAL4]* and *p[w+ prdGAL4]* (Brand and Perrimon, 1993); *p[w+,UAS-GMA]* (Bloor and Kiehart, 2001); *p[w+,RhoA^{N19}]* and *RhoA^{72O}* (Strutt et al., 1997); *p[w+,UAS-p35]* (Zhou et al., 1997); and the β-gal enhancer trap *puc^{E69}* (Ring and Martinez Arias, 1993).

Single or double combinations of transgenes were expressed in epidermal stripes by crossing either *w;p[w+,enGAL4]* or *w;p[w+,prdGAL4]* virgins to males of the following genotypes: *w;p[w+,UAS-GMA]*, *w;p[w+,RhoA^{N19}]*, *w;p[w+,UAS-GMA];p[w+,RhoA^{N19}]* or *w;p[w+,UAS-p35];p[w+,RhoA^{N19}]*. The puc^{E69} enhancer trap was co-expressed with $RhoA^{N19}$ by crossing *p[w+,enGAL4]/+; puc^{E69}/+* males to *w;p[w+,RhoA^{N19}]* virgins. The presence of *puc^{E69}* was detected by assaying expression of β-gal; $RhoA^{N19}$ expression was inferred by detection of epidermal stripes showing actin organization defects. Crosses were cultured in small population cages and eggs were collected on grape juice plates and aged at 25°C.

Further information can be obtained from FlyBase (http://flybase.bio.indiana.edu/).

Cuticle preparations

Two-hour egg collections were aged for 46 hours at 25°C. Unhatched, fertilized embryos were hand dechorionated and transferred to an agar slab where they were appropriately oriented. They were transferred to an embryo glue coated cover slip, covered with Hoyer's medium and placed on a glass slide. A small weight was placed over the cover slip and the slides were incubated at 65°C for 24 hours to allow embryonic tissues to clear and cuticles to flatten.

Immunofluorescence

Antibody staining was performed on whole embryos using standard methods with the exception of staining with the anti-nonmuscle myosin II heavy chain antibody, 656, which was performed as described (Bloor and Kiehart, 2001; Young et al., 1993).

Staining with rhodamine-phalloidin also followed standard methods with the exception that dechorionation was performed with 80% ethanol. Embryos were incubated for 2 hours at room temperature in a solution containing a rhodamine-phalloidin concentration of 4×10^{-4} units/μl.

The following primary antibodies were used in this study: a 1:1000 dilution of rabbit anti-nonmuscle myosin II heavy chain, 656 (Kiehart and Feghali, 1986; Kiehart et al., 1990), a 1:1000 dilution of mouse anti-β-gal (Roche Diagnostics Corporation, Indianapolis, IN), a 1:125 dilution of rat anti-DE-cadherin, DCAD2 (Oda et al., 1994) and a 1:25 dilution of rabbit anti-β_{Heavy}-spectrin, 243 (Thomas and Kiehart, 1994). Affinity-purified, directly conjugated fluorescent secondary antibodies from commercial sources were used at the following concentrations: FITC-conjugated anti-mouse, 1:1000; rhodamine-conjugated anti-rabbit, 1:1000; CY3-conjugated anti-rat, 1:2000.

Microscopy

Digital images of cuticle preparations were collected on a Spot camera (Diagnostic Instruments, Sterling Heights, MI) mounted on a Zeiss Axioplan using a 20×, 0.5 NA objective. Confocal microscopy for fixed specimens was performed either with a Zeiss LSM410 and Axiovert S100 TV or a Zeiss LSM510 and Axioplan 2 using 25×, 0.8 NA, 40×, 0.9 NA and 63×, 1.4 NA objectives. Live embryos were imaged using a modified Teflon window chamber (Kiehart et al., 1994) and a Perkin Elmer Ultraview Confocal Scanner fitted to a Zeiss Axioplan with a 40×, 1.2 NA objective. Images were collected every 30 seconds on a Sony Ultrapix CCD camera. Images were processed in Adobe Photoshop (Adobe Systems, San Jose, CA); videos were processed using NIH Image (http://rsb.info.nih.gov/nih-image/).

RESULTS

We have investigated RhoA function in the developing embryonic epidermis of *Drosophila* by using the GAL4/UAS system (Brand and Perrimon, 1993) to express the dominant-negative *RhoA^{N19}* construct in stripes of epidermal cells. This approach has two advantageous features. First, RhoA^{N19} expression should be limited to the developing epidermis; secondly, in fixed samples the phenotype of RhoA^{N19}-expressing epidermal cells can be directly compared with wild-type epidermal cells within the same embryo.

In this study, we used two GAL4 drivers, *enGAL4* and *prdGAL4*, to drive expression in epidermal stripes. To test whether expression driven by these GAL4 lines is limited to the epidermis, we first used them to express GMA, an actin marker in which GFP is fused to the *Drosophila* Moesin actin-binding domain (Bloor and Kiehart, 2001; Edwards et al., 1997; Kiehart et al., 2000). By following GFP fluorescence in live wild-type embryos, we find that both GAL4 lines drive expression in epidermal stripes from before germband extension through dorsal closure (Fig. 1A-C). The *enGAL4* driver directs GMA expression in 14, narrow epidermal stripes, while *prdGAL4* driven GMA expression remains in eight wide stripes throughout dorsal closure. In neither case does GMA expression exactly recapitulate the expression pattern of the endogenous genes, most probably because of the high stability of GMA (Edwards et al., 1997). In addition, both GAL4 lines drive variable GMA expression in some amnioserosa cells, although this is more apparent with *prdGAL4* (Fig. 1B,C; see Movie 1 at http://dev.biologists.org/supplemental/). Prior to germband elongation, both *en* and *prd* are expressed in the dorsal ectoderm (DiNardo et al., 1985; Kilchherr et al., 1986), the tissue fated to become the amnioserosa. This amnioserosal expression is again likely to be an effect of GMA stability. Interestingly, the amnioserosal cells that express GMA always lie above and continue dorsally the epidermal stripe of GAL4-driven expression (Fig. 1B,C). Furthermore, during germband retraction they move in register with their corresponding epidermal stripe (see Movie 1 at http://dev.biologists.org/supplemental/). Importantly however, as dorsal closure begins, amnioserosal expression fades, leaving a pattern of stripes restricted to the epidermis.

At the beginning of dorsal closure GMA expression, driven

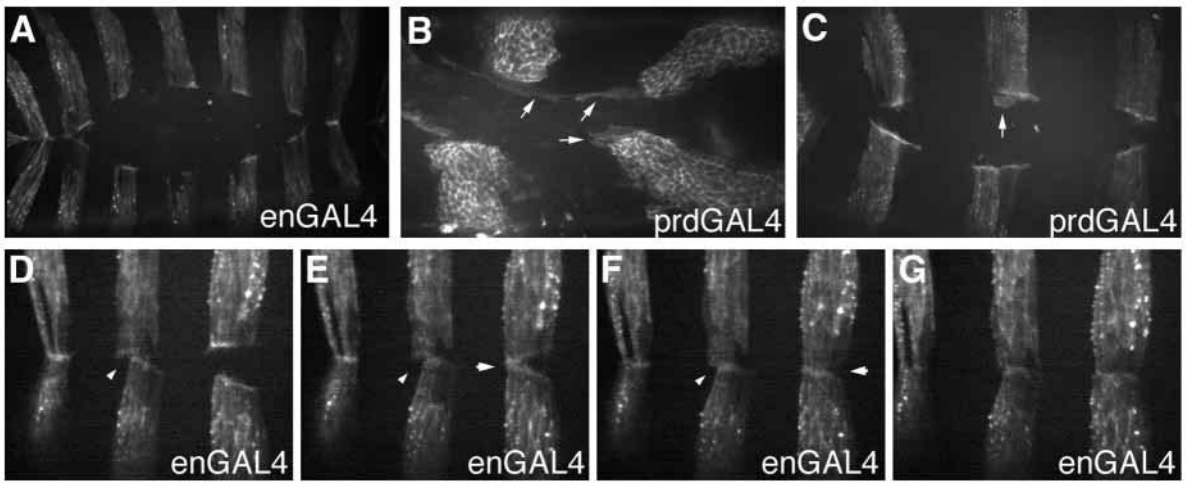

Fig. 1. Striped epidermal expression of GMA reveals cell shape during morphogenesis. *UAS-GMA* expression driven by either *enGAL4* (A,D-G) or *prdGAL4* (B,C) demonstrates cell shape in epidermal stripes, as well as in some amnioserosal cells (arrows in B,C) that continue these stripes dorsally. (D-G) Frames from a time-lapse video (Movie 1 at http://dev.biologists.org/supplemental/) showing that epidermal stripes generally meet in register at the dorsal midline. However, mismatches are observed (small arrowheads in D-F) and in some cases suturing along the dorsal midline continues for a substantial distance prior to mismatch resolution (E,F, arrows indicate progression of dorsal closure).

by either GAL4 line, clearly demonstrates a parallel band of actin at the leading edge, as well as dorsally extending filopodia (Movie 2 at http://dev.biologists.org/supplemental/). Leading edge cells, followed by lateral epidermal cells, then extend dorsally as closure proceeds. As opposing stripes come together at the dorsal midline, leading edge filopodia from opposite epidermal hemispheres appear to adhere and rapidly pull the epidermal fronts together as previously reported (Jacinto et al., 2000). However, we observe frequent initial mismatches between opposing stripes (Fig. 1D; see Movie 2 at http://dev.biologists.org/supplemental/). These are always resolved, but resolution can occur after dorsal closure has extended well beyond the mismatched stripes (Fig. 1E-G), suggesting that opposing epidermal cells can adjust their relative positions at the dorsal midline subsequent to closure.

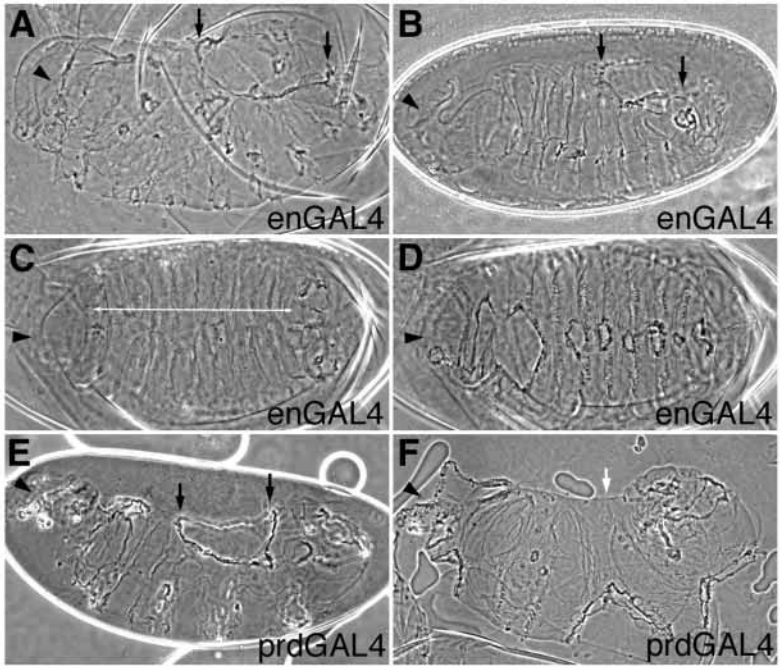

Fig. 2. RhoA^{N19} expression disrupts dorsal closure and ventral integrity. *UAS-RhoA^{N19}* expression using either *enGAL4* (A-D) or *prdGAL4* (E,F), causes defects in the dorsal and ventral cuticle. All embryos exhibit anterior holes (arrowheads) and some sort of lateral scarring. Expression of RhoA^{N19} (A,E), and co-expression with GMA (B) can result in the formation of a posteriorly located dorsal hole (arrows indicate extent of the hole). Alternatively embryos exhibit puckering at the dorsal midline (C,F; white arrows indicates dorsal midline) and ventral cuticular holes (D,F).

RhoA^{N19} disrupts dorsal closure and ventral epidermal integrity

To determine the effect of expressing RhoA^{N19} in epidermal stripes, we crossed virgin females homozygous for either *enGAL4* or *prdGAL4* to males homozygous for *UAS-RhoA^{N19}*. In both cases no embryos were observed to hatch (n=123 and 219 embryos, respectively), demonstrating that striped expression of RhoA^{N19} causes embryonic lethality. Cuticle preparations show that each GAL4 line generates a similar, but distinct terminal phenotype (Fig. 2A-F). All embryos have a large anterior hole, indicating failure of head involution and reflecting a GAL4-driven stripe of expression in the head ectoderm, as well as variable lateral, ventral and dorsal defects. Regardless of the GAL4 driver used, ~40% of embryos have a hole in the dorsal cuticle (Fig. 2A,B,E), indicative of a disruption in dorsal closure. The rest exhibit puckering at the dorsal midline (Fig. 2C,F), which probably represents a defect in the suturing stage of dorsal closure. GAL4-specific differences in phenotype relate to the magnitude of the dorsal and ventral defects. RhoA^{N19} expression driven by *enGAL4* generates small ventral holes (Fig. 2D) and posteriorly positioned dorsal holes (Fig. 2A,B) that range in size from single segments to the length of the embryo. By contrast, embryos that express RhoA^{N19} under the control of *prdGAL4* exhibit wide ventral holes that extend laterally, frequently merging with the lateral defects (Fig. 2F). Furthermore, the dorsal holes exhibited by these embryos, while still posteriorly positioned, never extend the length of the embryo. These differences probably reflect the different expression patterns of the two GAL4 lines. Interestingly, with both GAL4 lines we observe a reverse correlation between the size of the dorsal cuticular hole and that of the ventral holes: the larger the dorsal hole, the smaller the ventral holes (compare Fig. 2A,B with 2C,D and compare 2E with 2F).

RhoA^{N19} disrupts epidermal cell morphology and cytoskeletal organization

As RhoA regulates actin organization and activation of nonmuscle myosin II, disruption of its function during dorsal closure might be expected to affect localization of actin and nonmuscle myosin II both at the leading edge and in the lateral epidermis. To test this hypothesis, we first stained embryos expressing RhoA^{N19} via *prdGAL4* or *enGAL4* with rhodamine-phalloidin to visualize F-actin distribution (Fig. 3). At germband retraction stages, cell shape is clearly abnormal within stripes of RhoA^{N19} expression (Fig. 3A,B). RhoA^{N19}-expressing epidermal cells possess apical filopodia and appear generally larger and more rounded than cells in stripes of wild-type tissue. By comparing optical, confocal sections at the surface (Fig. 3A) with sections deeper within the epithelium (Fig. 3B), it is clear that some cells at the surface have flattened and spread over underlying RhoA^{N19}-expressing cells and neighboring wild-type epidermis. After completion of germband retraction, but prior to the formation of the leading edge actomyosin purse string, RhoA^{N19}-expressing leading edge cells put out extensive filopodia (Fig. 3C) and these become more prominent as dorsal closure progresses (Fig. 3D-G). During dorsal closure, wild-type leading edge cells possess a clear band of actin that runs parallel to the leading edge. In addition, small spikes of staining (under these fixation conditions, we observe approx. two for every five wild-type leading edge cells, averaging ~4 μm in length, n=7) extend perpendicular to the leading edge, presumably representing leading edge filopodia. The leading edge cells within stripes of RhoA^{N19} expression do not possess an organized band of actin. However, filopodal spikes are both more common (averaging one per cell) and larger (averaging 8.4 μm, n=12).

Staining these embryos with an antibody that specifically

recognizes nonmuscle myosin II heavy chain demonstrates that RhoA^{N19} expression also causes defects in nonmuscle myosin II localization (Fig. 4). This is first seen at stage 11, where RhoA^{N19}-expressing mesectodermal cells fail to invaginate at the ventral midline (Fig. 4A) and instead spread along the midline groove generated by the invagination of their wild-type neighbors. Within these cells, nonmuscle myosin II staining is partially lost from the cell cortex and is more cytoplasmic (Fig. 4B). This defect in localization is more distinct in later embryos undergoing dorsal closure (Fig. 4C-F). At these stages and particularly at the leading edge, RhoA^{N19}-expressing cells lose much of their cortically localized nonmuscle myosin II. Instead, although excluded from the nucleus, it is present diffusely within the cytoplasm (Fig. 4C,E). The leading edge cells also show clear differences in cell morphology when compared with wild-type neighbors. They appear to spread dorsally over the amnioserosa (Fig. 4C,E) and laterally, such that connections are made between adjacent RhoA^{N19}-expressing stripes (Fig. 4D,F).

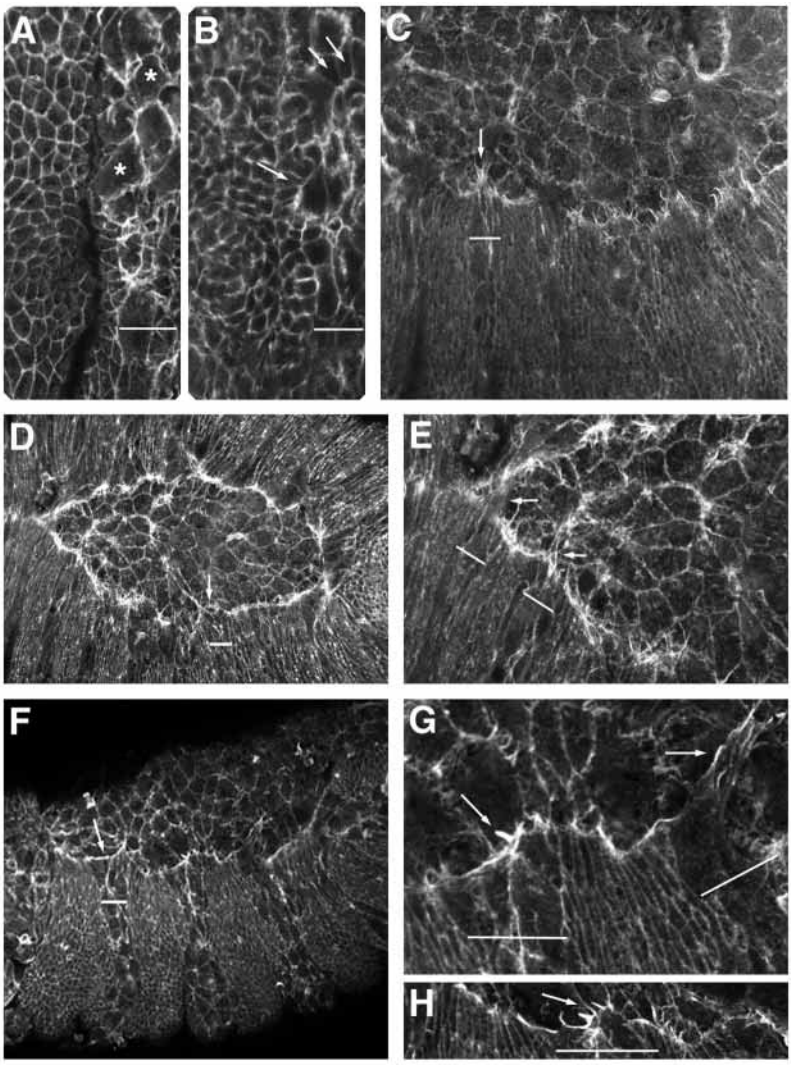

Fig. 3. RhoA^{N19} expression disrupts actin organization and epidermal cell morphology. Embryos expressing *UAS-RhoA^{N19}* under the control of *prdGAL4* (A,B,F-H) or *enGAL4* (C-E) stained with rhodamine-phalloidin to reveal F-actin. In each panel, white bars indicate representative stripes of RhoA^{N19} expression. (A,B) Two focal planes of the same high magnification lateral field from a stage 12 embryo undergoing germband retraction; RhoA^{N19}-expressing cells within the *prdGAL4* stripe have flattened and spread (indicated by asterisks in A) over each other and wild-type epidermis (indicated by arrows in B). (C) Stage 13 embryo prior to dorsal closure, extensive filopodia emanate from RhoA^{N19}-expressing leading edge cells (arrow). Leading edge cells expressing RhoA^{N19} (D,F) or co-expressing RhoA^{N19} and GMA (H) appear to extend across the amnioserosa and continue to put out extensive filopodia (arrows) as dorsal closure proceeds. These filopodia (arrows) are easily seen at higher magnification (E,G,H).

RhoA inhibits JNK signaling

The effect of RhoA^{N19} on the organization of actin and nonmuscle myosin II in the leading edge could be due to disruption of the JNK pathway. However, it has been reported that expression of RhoA^{N19} within the leading edge has no effect on JNK-dependent *dpp* expression (Lu and Settleman, 1999). The *puc^{E69}* enhancer trap directs expression of β-gal exclusively in the leading edge (Fig. 5A) in a manner that is dependent on JNK signaling (Martin-Blanco et al., 1998). Thus, we assayed *puc^{E69}* directed β-gal expression in embryos expressing RhoA^{N19} under the control of *enGAL4*. These embryos express β-gal in all the cells of the leading edge. However, within stripes of RhoA^{N19} expression, β-gal can also be detected in cells just lateral to the leading edge (Fig. 5B,C). We have shown that RhoA^{N19} expression causes cell rearrangement, thus the presence of β-gal-positive cells in the lateral epidermis could reflect rearrangement of leading edge cells. Alternatively, these cells could be lateral epidermal cells that now ectopically express *puc*. Each stripe of *enGAL4* driven GMA expression is five cells wide at the leading edge. By counting β-gal-positive nuclei in our experimental embryos, we find that up to 10 cells are labeled with β-gal in individual RhoA^{N19} expression stripes (Fig. 5C). In other words, the number of β-gal-positive nuclei present within a domain of RhoA^{N19} expression can be greater than the number of leading edge cells in that domain. Furthermore, we detected β-gal-positive cells within the ventral epidermis (Fig. 5D). We conclude that, although cell rearrangement is certainly a factor, RhoA^{N19} can induce ectopic *puc* expression. This suggests that in the absence of RhoA function the JNK signaling pathway can become ectopically activated in the lateral and ventral epidermis.

RhoA^{N19} affects epidermal cell behavior

To determine the effect of RhoA^{N19} expression on epidermal cell shape and F-actin distribution in real time, we co-expressed GMA and RhoA^{N19} using either *enGAL4* or *prdGAL4*. Similar observations were made with both GAL4 lines. At the leading edge the most striking defect is the formation of ectopic cell ‘bridges’ that link stripes of RhoA^{N19}-expressing cells. In some embryos, these appear during germband retraction (Fig. 6A; see Movie 3 at http://dev.biologists.org/supplemental/). As posterior segments

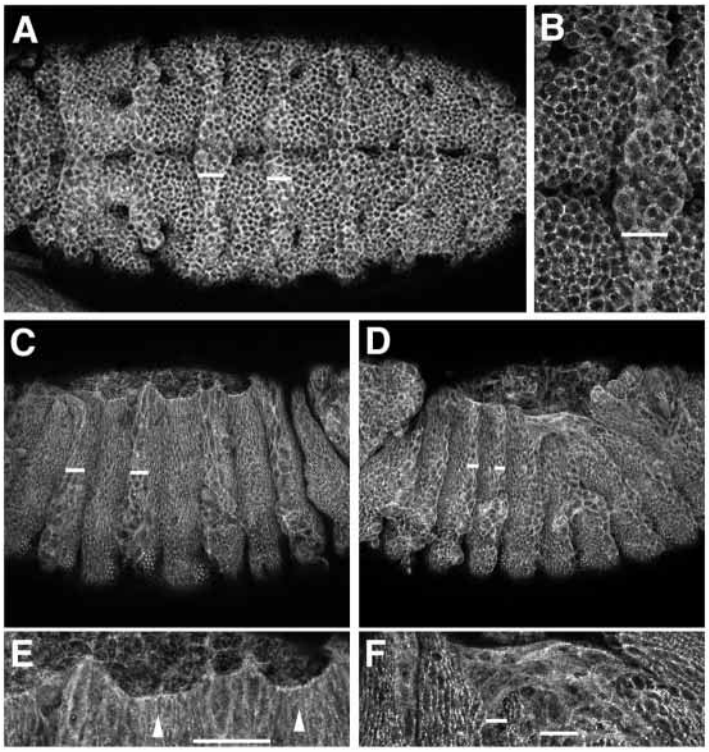

Fig. 4. RhoA^{N19} disrupts nonmuscle myosin II localization. Embryos expressing *UAS-RhoA^{N19}* under the control of *enGAL4* (A,B,D,F) or *prdGAL4* (C,E) were stained for nonmuscle myosin II. In all panels, bars indicate the extent of representative RhoA^{N19}-expressing stripes. (A,B) During germband retraction, cells expressing RhoA^{N19} fail to ingress at the ventral midline and rather bulge, anteriorly and posteriorly, along the groove formed by neighboring wild-type cells. At higher magnification (B), nonmuscle myosin II appears less cortical and more cytoplasmic when compared with wild type. (C,E) During dorsal closure, nonmuscle myosin II is no longer highly concentrated at the leading edge of RhoA^{N19} stripes and these cells seem to spread forward over the amnioserosa. Arrowheads in the high-magnification view (E) indicate wild-type nonmuscle myosin II localization. (D,F) Leading edge cells expressing RhoA^{N19} also extend laterally, forming cell bridges. At this stage, cortical nonmuscle myosin II is clearly reduced in RhoA^{N19}-expressing cells.

retract, dorsal epidermal cells constrict, allowing them to make a tight turn around the end of the embryo. This constriction does not occur in RhoA^{N19}-expressing stripes. Thus, when intervening wild-type cells constrict, leading edge cells from RhoA^{N19}-expressing stripes come into close proximity. Filopodia extending from these cells then initiate ectopic cell contacts. Whether or not these early ectopic contacts occur, extensive and dynamic dorsally oriented filopodia project from the leading edge of RhoA^{N19}-expressing stripes prior to the start of dorsal closure, consistent with our observations on fixed embryos (Fig. 6B, compare to Fig. 3C). As dorsal closure proceeds, RhoA^{N19}-expressing leading edge cells spread over the amnioserosa, while continuing to extend long filopodia (Fig. 6C). As in the wild type leading edge, these filopodia continuously probe their embryonic environment. However, they are not restricted in their adhesive behavior. In wild-type leading edge cells, filopodia only make adhesive contacts with their counterparts from the opposite epidermal hemisphere (see Movie 2 at http://dev.biologists.org/supplemental/) (Jacinto et al., 2000). When filopodia from RhoA^{N19}-expressing stripes touch, either during germband retraction or dorsal closure, they form ectopic cell contacts (Fig. 6D-F; see Movie 4 at http://dev.biologists.org/supplemental/). Thus, when development in these embryos arrests, many stripes of RhoA^{N19}-expressing cells are connected at the leading edge.

Ventrally, RhoA^{N19}-dependent defects are first seen at the ventral midline. Normally mesectodermal cells invaginate; however, within RhoA^{N19} expression stripes, invagination does not occur (Fig. 4A,B). Instead, actin within these and neighboring cells compacts, reminiscent of cells entering apoptosis (see Movie 5 at http://dev.biologists.org/supplemental/). To test the hypothesis that apoptosis underlies

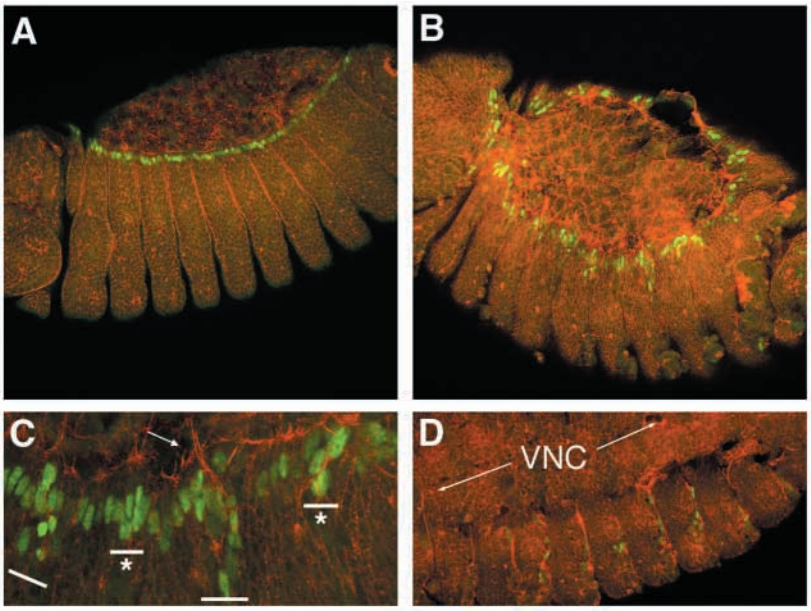

Fig. 5. Loss of RhoA function affects *puc* expression. (A) Lateral view of an embryo carrying the *puc^{E69}* enhancer trap, stained with rhodamine-phalloidin to detect F-actin and anti-β-gal antibody to detect *puc* expression. In wild-type embryos, *puc* expression is strictly limited to the single row of leading edge cells. (B-D) Embryos carrying the *puc^{E69}* enhancer trap and expressing RhoA^{N19} in *enGAL4* stripes, stained as above. (B) Dorsal view showing that, although the leading edge is ragged, *puc* expression occurs along its entire length. In some places, however, *puc* expression is seen away from the leading edge. (C) High-magnification view showing stripes of RhoA^{N19} expression (indicated by white bars and detected by abnormal actin organization, arrow) in which either cell rearrangement (stripes marked by an asterisk) or ectopic *puc* expression results in cells lateral to the leading edge being positive for β-gal staining. (D) Ectopic expression of *puc* is also detected within cells of the ventral epidermis.

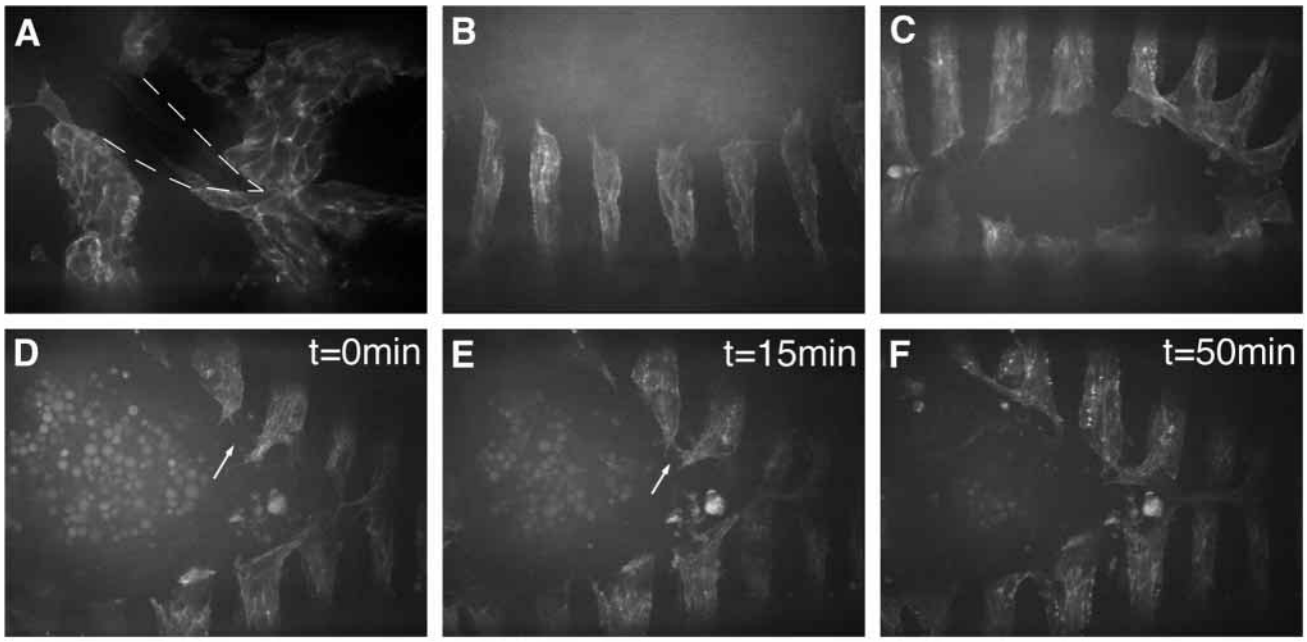

Fig. 6. RhoA^{N19} expression alters leading edge cell behavior. Lateral (A,B) and dorsal (C-F) views of embryos co-expressing *UAS-RhoA^{N19}* and *UAS-GMA* via *prdGAL4* (A) or *enGAL4* (B-F). In stage 12 embryos undergoing germband retraction, stripes of RhoA^{N19}-expressing cells do not narrow dorsally (A, compare with Fig. 1B; compare Movie 3 with Movie 1 at http://dev.biologists.org/supplemental/), bringing RhoA^{N19}-expressing stripes into close proximity and allowing leading edge filopodia to initiate cell bridge formation. Regardless of whether cell bridges are formed, extensive leading edge filopodia are clearly observed by the completion of germband retraction (B, compare with Fig. 3C). (C-F) Subsequently, RhoA^{N19}-expressing leading edge cells spread dorsally and laterally (C) and when filopodia come into contact (arrows), they form ectopic lateral cell-cell adhesions and cell bridges (D-F).

RhoA^{N19}-dependent loss of ventral epidermal integrity, we co-expressed RhoA^{N19} and the apoptosis inhibitor, p35 using the *enGAL4* driver. Embryos expressing RhoA^{N19} alone exhibit 5.4 ventral cuticular defects per embryo; co-expression of p35 reduced this number to 3.7 (n=24 and 21 respectively, P=0.011). This partial suppression suggests that, while programmed cell death contributes to RhoA^{N19}-dependent loss of ventral epidermal integrity, other mechanisms also play a role. Cells undergoing apoptosis are clustered close to the ventral midline, slightly more lateral cells are unaffected. However, at later stages these cells occasionally drop out of the epidermal epithelial layer (see Movie 6 at http://dev.biologists.org/supplemental/). Furthermore, RhoA^{N19}-expressing cells that remain within the epithelium no longer adhere tightly to each other. This is demonstrated by the ability of hemocytes, highly migratory phagocytotic cells, to transmigrate between these cells (see Movie 6 at http://dev.biologists.org/supplemental/) thereby generating or augmenting defects within the epidermal layer. Thus, even in the presence of p35, ventral cuticular defects may result from RhoA^{N19}-expressing epidermal cells losing contact with each other and falling out of the epidermis.

RhoA^{N19} affects epidermal cell-cell adhesion and cell polarity

Clearly RhoA^{N19}-expressing epidermal cells exhibit altered adhesive properties. Cell-cell adhesion in the *Drosophila* embryonic epidermis is mediated by DE-cadherin. To test whether the altered adhesive properties of RhoA^{N19}-expressing cells are accompanied by changes in DE-cadherin mediated cell-cell adhesion, we stained embryos expressing RhoA^{N19} via *enGAL4* with an antibody that specifically recognizes this adhesion molecule. In embryos undergoing dorsal closure, DE-cadherin is completely lost from the surface of all RhoA^{N19}-expressing cells both dorsally and ventrally (Fig. 7A-C), although surface staining persists on dorsal epidermal cells longer than it does on ventral cells. Indeed, defects in DE-cadherin localization are observed from stage 11 onwards (Fig. 7D). As DE-cadherin localizes to apical cell junctions (Uemura et al., 1996), loss of cell surface staining could be due to loss of cell polarity. In this scenario, DE-cadherin should become evenly distributed around the cell surface. However, epidermal cells expressing RhoA^{N19} no longer stain for DE-cadherin suggesting that failure to localize leads to its degradation. We also stained these embryos with an antibody that recognizes β_H-spectrin, a marker for the apicolateral domain of epidermal cells (Thomas and Kiehart, 1994). We observe clear apicolateral staining in wild-type epidermal cells; however, within stripes of RhoA^{N19} expression, β_H-spectrin is lost from this domain (Fig. 7E,F) and uniform weak staining can be observed all around the cell surface. This defect in β_H-spectrin localization is also initially observed at stage 11 (Fig. 7G). Thus, our data suggest that inhibition of RhoA function results in loss of cell polarity, but do not distinguish between this being the result or the cause of DE-cadherin loss from the cell surface.

To determine whether loss of DE-cadherin was also a feature of zygotic *RhoA* mutants, we stained embryos homozygous for a severe *RhoA* allele with the DE-cadherin antibody. Maternally contributed RhoA supports early

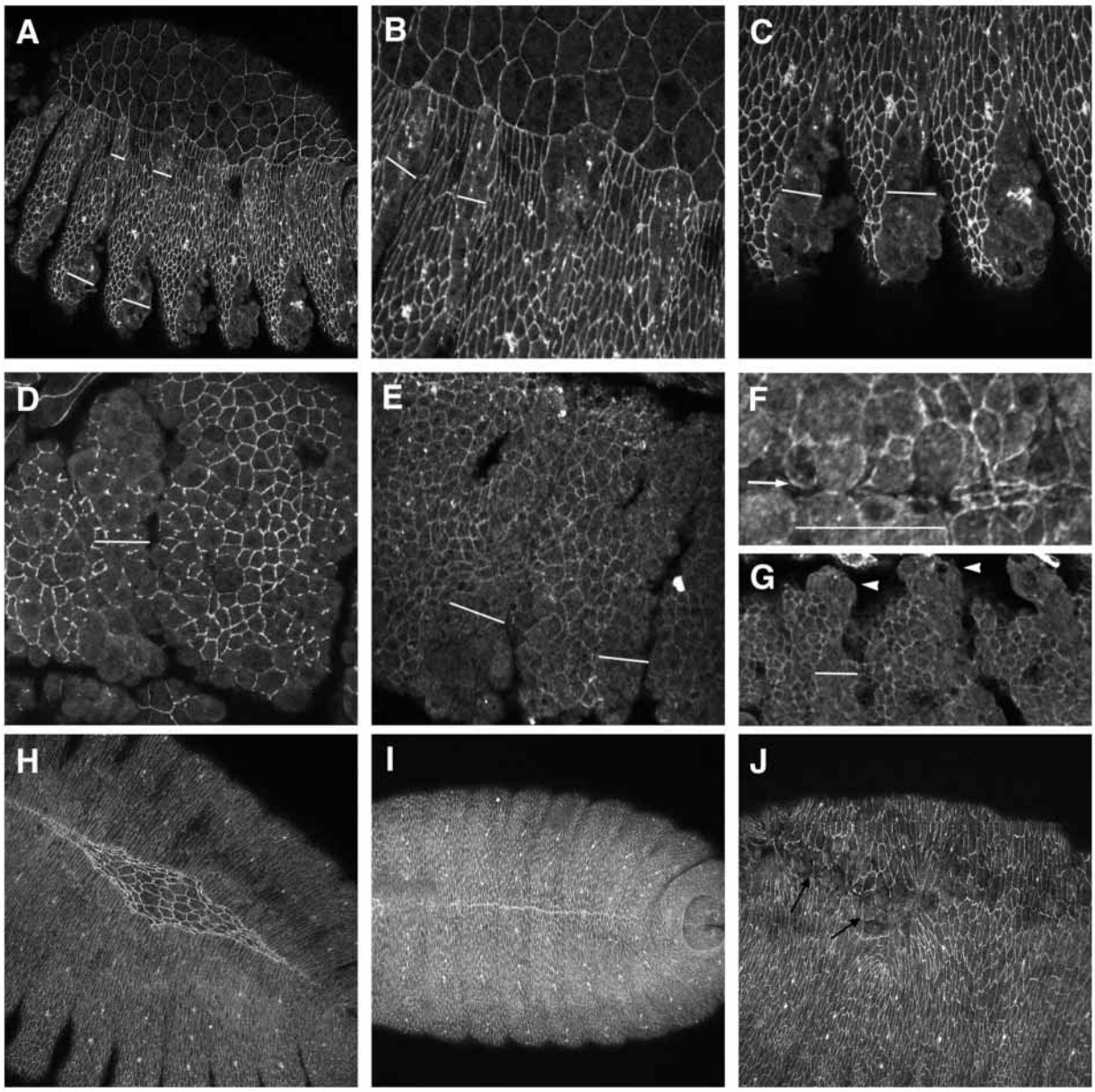

Fig. 7. Loss of RhoA function causes defects in DE-cadherin localization and epidermal cell polarity. Embryos expressing $RhoA^{N19}$ driven by *enGAL4* (indicated by bars) that were stained either with an antibody against DE-cadherin (A-D) or anti-β_{Heavy}-spectrin (E-G). (A) $RhoA^{N19}$ expression causes loss of cell surface DE-cadherin at dorsal closure stages. Higher magnification images show complete loss of DE-cadherin surface staining is first apparent in ventral epidermal cells (C), when compared with the dorsal epidermis (B). (D) At earlier stages, punctate spots of DE-cadherin staining fail to coalesce into bands of apical staining in cells expressing $RhoA^{N19}$. (E) Lateral view of a stage 12 embryo; $RhoA^{N19}$-expressing cells lose apicolateral staining of β_{Heavy}-spectrin. (F) Dorsal view of a stage 11 embryo showing loss of β_{Heavy}-spectrin in $RhoA^{N19}$-expressing stripes at the ventral midline (midline indicated by an arrow). (G) Later, loss of apicolateral staining is clearly seen in $RhoA^{N19}$-expressing leading edge cells (arrowheads) that push beyond wild type neighbors. (H) DE-cadherin staining of a stage-14 RhoA mutant embryo depicting leading edge disorganization, but no loss of DE-cadherin staining. (J) At stage 15, when dorsal closure is complete, some RhoA mutants exhibit loss of cell surface DE-cadherin at sites of dorsal puckering (arrows; compare with wild-type embryo, I).

development of these embryos and most complete dorsal closure. Despite this, mutant embryos can be detected by their clear head involution defects and disorganization of the leading edge (Fig. 7H). No defects in DE-cadherin localization are seen at this stage. However, *RhoA* mutant embryos that have completed dorsal closure exhibit leading edge puckering and this can be associated with loss of DE-cadherin staining (Fig. 7J).

DISCUSSION

Previous studies on RhoA function during dorsal closure have focused on its role in the formation of the leading edge actomyosin purse-string. Here we expand upon this initial work and show that RhoA is required for proper organization of actin and nonmuscle myosin II throughout the epidermis. In addition we find that inhibition of RhoA causes misregulation of the JNK

transcription activation pathway, loss of DE-cadherin from the cell surface and disruption of the apicolateral distribution of β_{Heavy}-spectrin. We find that these changes in cell physiology have differential effects on cell behavior that depend upon the position of the cell within the dorsal-ventral axis. In particular, cell-cell adhesion in the ventral and lateral epidermis is severely compromised, but at the leading edge $RhoA^{N19}$-expressing cells form new, ectopic cell-cell adhesions.

RhoA, actomyosin organization and contractility

Tension generated in the amnioserosa and the leading edge of the lateral epidermis independently contributes to the forces that drive dorsal closure (Kiehart et al., 2000). It has been proposed that nonmuscle myosin II activation generates tension in the leading edge and that this causes a leading edge intracellular actomyosin purse-string to shorten (Young et al., 1993). Signaling downstream of RhoGTPase activates nonmuscle myosin II by modulating the level of myosin regulatory light chain phosphorylation (reviewed by Bresnick, 1999). As such, expression of $RhoA^{N19}$ in epidermal stripes might disrupt contraction of the leading edge purse-string. In our experiments, defects in actin and nonmuscle myosin II organization caused by $RhoA^{N19}$ expression are first observed at germband extension, up to 2 hours before purse-string formation. Thus, while actin and nonmuscle myosin II are localized at the leading edge in wild-type tissue, a purse-string structure is never formed in leading edge cells that express $RhoA^{N19}$. $RhoA^{N19}$ expression therefore effectively cuts the leading edge purse-string at multiple sites. We find that this does not necessarily prevent progression of dorsal closure, confirming previous experiments that demonstrate that the integrity of the leading edge is not required for dorsal closure to continue to completion (Kiehart et al., 2000). We conclude that small independent regions of leading edge in wild-type epidermal stripes can, in conjunction with contraction of the amnioserosa, migrate dorsally with relative normalcy.

The question that arises is how do epidermal cells expressing $RhoA^{N19}$ move dorsally in the absence of a leading edge purse-string? These cells could hitchhike, i.e. they are pulled dorsally by the amnioserosa or dragged along with neighboring wild-type cells. We show that, although spread and disorganized, dorsal $RhoA^{N19}$-expressing cells do maintain adhesion with wild-type neighbors and this might then allow passive $RhoA^{N19}$-expressing cells to move dorsally with wild-type tissue. This is consistent both with the inverse correlation between integrity of the ventral epidermis and the extent to which dorsal closure proceeds, as well as with our observations on the distribution of tension at the embryo surface during dorsal closure (Kiehart et al., 2000). Thus, as the epidermis lateral to the leading edge opposes dorsal closure, ventral failure of epidermal integrity (and hole formation) would release the tensional restraints on the remaining lateral epidermis, allowing it to move dorsally with more success. Similarly, in the absence of this release (i.e. the ventral epidermis retains its integrity and opposes dorsal movement of the epidermis), the leading edge is presumably no longer capable of generating sufficient force to drive dorsal closure to completion.

RhoA and the regulation of transcription in the leading edge

We demonstrate that $RhoA^{N19}$ expression causes ectopic activation of the JNK pathway in the lateral epidermis, suggesting that RhoA normally functions to inhibit JNK signaling. JNK activation is antagonized by the protein phosphatase encoded by *puc*, and in *puc* mutants JNK signaling is increased at the leading edge and is activated in the lateral epidermis (Martin-Blanco et al., 1998). Thus, JNK signaling in wild-type embryos is not maximal and basal JNK activity in the lateral epidermis is revealed in the absence of either *puc* or RhoA mediated repression. Interestingly, $RhoA^{N19}$ expression does not increase JNK signaling in the leading edge. This difference between the effect of *puc* mutations and $RhoA^{N19}$ expression could be due to ectopic $RhoA^{N19}$ suppressing an upstream JNK activator that is itself maximally activated in the leading edge.

RhoA and epidermal cell adhesion

Co-expression of $RhoA^{N19}$ and GMA demonstrates that, in addition to effects on the actin cytoskeleton, inhibition of RhoA has profound effects on the adhesive properties of epidermal cells. In accordance with this, we show that DE-cadherin is lost from the surface of $RhoA^{N19}$-expressing cells. Rho is required for E-cadherin-mediated epithelial cell-cell adhesion in cultured vertebrate cells: in keratinocytes and MDCK cells, blocking Rho function prevents formation of E-cadherin-based junctions and causes preformed junctions to breakdown (Braga et al., 1999; Braga et al., 1997; Takaishi et al., 1997). This effect is dependent on cell-cell junction maturity; blocking Rho causes E-cadherin to be lost rapidly (within 1 hour) from immature junctions, but E-cadherin can persist for several hours at mature junctions. We also observe this differential affect, as removal of DE-cadherin from the cell surface is not uniform throughout the $RhoA^{N19}$-expressing stripe; ventral cells lose surface staining sooner than dorsal cells. This most probably reflects regional differences in the maturity of epidermal cell junctions. Cells of the dorsal epidermis form a compact epithelium early in stage 10, while neuroblast delamination in the ventral neurectoderm delays formation of the ventral epidermis proper until well into stage 11, by which time *enGAL4*- and *prdGAL4*-driven protein expression is apparent. Alternatively, the differential effect might be due to a dorsoventral gradient in *enGAL4*- or *prdGAL4*-driven expression of $RhoA^{N19}$. This seems unlikely, as no regional differences in fluorescence are observed when these GAL4 lines are used to drive GMA expression.

Drosophila E-cadherin is encoded by *shotgun* (*shg*) (Tepass et al., 1996; Uemura et al., 1996). If the primary defect associated with the epidermal expression of $RhoA^{N19}$ is loss of DE-cadherin, then the phenotypes induced by $RhoA^{N19}$ should phenocopy those of *shg* mutants. The defects exhibited by *shg* embryos are difficult to compare with those shown by embryos expressing $RhoA^{N19}$ in epidermal stripes. However, genetic analysis of *shg* demonstrates that the embryonic dorsal epidermis is less sensitive than the presumptive ventral epidermis to a reduction in DE-cadherin levels (Tepass et al., 1996; Uemura et al., 1996); embryos mutant for null *shg* alleles are missing head and ventral cuticle, while the dorsal cuticle appears unaffected. Thus, as with epidermal expression of $RhoA^{N19}$, *shg* mutants disrupt ventral epidermal integrity and cells undergo apoptosis, while dorsally epidermal cells remain adherent and secrete cuticle. However, there is at least one clear distinction between the genetic reduction of DE-cadherin and

the defects induced by expression of RhoA^{N19}. That is, both null and dominant-negative mutations in *shg* do not affect epithelial cell polarity (Tepass et al., 1996), while inhibition of RhoA activity does. It seems likely that this difference reflects the additional function of RhoA in generating cell polarity, possibly through organization of the actin cytoskeleton. We conclude that the epidermal defects caused by RhoA^{N19} expression cannot be explained simply on the basis of loss of DE-cadherin mediated adhesion.

Epidermal cell-cell adhesion in the absence of RhoA function

Maintenance of dorsal epithelial integrity in the absence of detectable surface DE-cadherin suggests that a secondary adhesion system must function in the dorsal epidermis. As in vertebrate cells different classical cadherins exhibit cell type dependent sensitivity to Rho inhibition (Braga et al., 1999) this could involve another member of the cadherin family. The possibility that two cell-cell adhesion systems function in the dorsal epidermis may explain the behavior of RhoA^{N19}-expressing cells. Embryos that express RhoA^{N19} in epidermal stripes differ from *shg* mutants in the uniformity of DE-cadherin loss from the cell surface. In *shg* mutants, zygotic DE-cadherin is lost from all cells, while striped expression of RhoA^{N19} results in two populations of dorsal epidermal cells, those with cell surface DE-cadherin and those without. Differential adhesion properties of cell populations are the molecular basis for the classical phenomenon of cell sorting. Thus, the ectopic cell bridges formed by RhoA^{N19}-expressing cells in our experimental embryos could be due to activation of a cell sorting mechanism between populations of dorsal epidermal cells that associate via different adhesion molecules.

In summary, by expressing the dominant negative RhoA^{N19} construct in epidermal stripes in the developing *Drosophila* embryo, we show that the small GTPase Rho has multiple functions throughout this tissue. It is therefore clear that experiments designed to test the function of Rho family GTPases in the epidermis cannot be interpreted simply in terms of their effect on the leading edge. The challenge ahead lies in dissecting the pathways downstream of Rho and determining how these Rho-dependent processes contribute individually to epidermal function and morphogenesis.

We thank Amy Bejsovec, Olga Nikiforova, Marek Mlodzic and Masatoshi Takeichi for the gift of fly stocks and antibodies. We thank Jackie Swain, Rick Fehon, Amy Bejsovec and Paul Martin for critical reading of the manuscript. This work was supported by NIH grants GM33830 and GM61240, as well as grants from the March of Dimes and Muscular Dystrophy Association awarded to D. P. K.

REFERENCES

Affolter, M., Nellen, D., Nussbaumer, U. and Basler, K. (1994). Multiple requirements for the receptor serine/threonine kinase *thick veins* reveal novel functions of TGFβ homologs during *Drosophila* embryogenesis. *Development* **120**, 3105-3107.

Arora, K., Dai, H., Kazuko, S., Jamal, J., O'Connor, M. and Letsou, A. (1995). The *Drosophila schnurri* gene acts in the Dpp TGFβ signaling pathway and encodes a transcription factor homologous to the human MBP family. *Cell* **81**, 781-790.

Bloor, J. W. and Kiehart, D. P. (2001). *zipper* nonmuscle myosin-II functions downstream of PS2 integrin in *Drosophila* myogenesis and is necessary for myofibril formation. *Dev. Biol.* **239**, 215-228.

Braga, V. M. M., Machesky, L. M., Hall, A. and Hotchin, N. A. (1997). The small GTPases Rho and Rac are required for the establishment of cadherin-dependent cell-cell contacts. *J. Cell Biol.* **137**, 1421-1431.

Braga, V. M. M., Del Maschio, A., Machesky, L. and Dejana, E. (1999). Regulation of cadherin function by Rho and Rac: modulation by junction maturation and cellular context. *Mol. Biol. Cell* **10**, 9-22.

Brand, A. H. and Perrimon, N. (1993). Targeted gene expression as a means of altering cell fates and generating dominant phenotypes. *Development* **118**, 401-415.

Bresnick, A. R. (1999). Molecular mechanisms of nonmuscle myosin-II regulation. *Curr. Opin. Cell Biol.* **11**, 26-33.

Brummel, T., Twombly, V., Marques, G., Wrana, J., Newfeld, S., Attisano, L., Massague, J., O'Connor, M. and Gelbart, W. (1994). Characterization and relationship of Dpp receptors encoded by the *saxophone* and *thick veins* genes in *Drosophila*. *Cell* **78**, 251-261.

Coso, O. A., Chiariello, M., Yu, J.-C., Teramoto, H., Crespo, P., Xu, N., Miki, T. and Gutkind, J. S. (1995). The small GTP-binding proteins Rac1 and Cdc42 regulate the activity of the JNK/SAPK signaling pathway. *Cell* **81**, 1137-1146.

Cote, S., Preiss, A., Haller, J., Schuh, R., Kienlin, A., Siefert, E. and Jackle, H. (1987). The *gooseberry-zipper* region of *Drosophila*: five genes encode different spatially restricted transcripts in the embryo. *EMBO J.* **6**, 2793.

DiNardo, S., Kuner, J. M., Theis, J. and O'Farrell, P. H. (1985). Development of embryonic pattern in *Drosophila melanogaster* as revealed by accumulation of the nuclear engrailed protein. *Cell* **43**, 59-69.

Edwards, K. A. and Kiehart, D. P. (1996). *Drosophila* nonmuscle myosin II has multiple essential roles in imaginal disc and egg chamber morphogenesis. *Development* **122**, 1499-1511.

Edwards, K. A., Demsky, M., Montague, R. A., Weymouth, N. and Kiehart, D. P. (1997). GFP-Moesin illuminates actin cytoskeleton dynamics in living tissue and demonstrates cell shape changes during morphogenesis in *Drosophila*. *Dev. Biol.* **191**, 103-117.

Genova, J. L., Jong, S., Camp, J. T. and Fehon, R. G. (2000). Functional analysis of Cdc42 in actin filament assembly, epithelial morphogenesis, and cell signaling during *Drosophila* development. *Dev. Biol.* **221**, 181-194.

Glise, B. and Noselli, S. (1997). Coupling of Jun amino-terminal kinase and Decapentaplegic signaling pathways in *Drosophila* morphogenesis. *Genes Dev.* **11**, 1738-1747.

Glise, B., Bourbon, H. and Noselli, S. (1995). *hemipterous* encodes a novel *Drosophila* MAP kinase kinase, required for epithelial cell sheet movement. *Cell* **83**, 451-461.

Grieder, N., Nellen, D., Burke, R., Basler, K. and Affolter, M. (1995). *Schnurri* is required for *Drosophila* Dpp signaling and encodes a zinc finger protein similar to the mammalian transcription factor PRDII-BF1. *Cell* **81**, 791-800.

Halsell, S. R. and Kiehart, D. P. (1998). 4ond-site noncomplementation identifies genomic regions required for *Drosophila* nonmuscle myosin function during morphogenesis. *Genetics* **148**, 1845-1863.

Halsell, S. R., Chu, B. I. and Kiehart, D. P. (2000). Genetic analysis demonstrates a direct link between Rho signaling and nonmuscle myosin function during *Drosophila* morphogenesis. *Genetics* **155**, 1253-1265.

Harden, N., Loh, H. Y., Chia, W. and Lim, L. (1995). A dominant inhibitory version of the small GTP-binding protein RAC disrupts cytoskeletal structures and inhibits developmental cell shape changes in *Drosophila*. *Development* **121**, 903-914.

Harden, N., Ricos, M., Ong, Y. M., Chia, W. and Lim, L. (1999). Participation of small GTPases in dorsal closure of the *Drosophila* embryo: distinct roles for Rho subfamily proteins in epithelial morphogenesis. *J. Cell Sci.* **112**, 273-284.

Hariharan, I. K., Hu, K. Q., Asha, H., Quintanilla, A., Ezzell, R. M. and Settleman, J. (1995). Characterization of Rho GTPase family homologues in *Drosophila melanogaster*: overexpressing Rho1 in retinal cells causes a late developmental defect. *EMBO J.* **14**, 292-302.

Hou, X. S., Goldstein, E. S. and Perrimon, N. (1997). *Drosophila* Jun relays the Jun amino-terminal kinase signal transduction pathway to the Decapentaplegic signal transduction pathway in regulating epithelial cell sheet movement. *Genes Dev.* **11**, 1728-1737.

Jacinto, A., Wood, W., Balayo, T., Turmaine, M., Martinez-Arias, A. and Martin, P. (2000). Dynamic actin-based epithelial adhesion and cell matching during *Drosophila* dorsal closure. *Curr. Biol.* **10**, 1420-1426.

Karess, R. E., Chang, X., Edwards, K. A., Kulkarni, S., Aguilera, I. and Kiehart, D. P. (1991). The regulatory light chain of nonmuscle myosin is

encoded by *spaghetti-squash*, a gene required for cytokinesis in *Drosophila*. *Cell* **65**, 1177-1189.

Kiehart, D. P. and Feghali, R. (1986). Cytoplasmic myosin from *Drosophila melanogaster*. *J. Cell Biol.* **103**, 1517-1525.

Kiehart, D. P., Ketchum, A., Young, P., Lutz, D., Alfenito, M. R., Chang, X.-j., Awobuluyi, M., Pesacreta, T. C., Inoue, S., Stewart, C. T. et al. (1990). Contractile proteins in *Drosophila* development. *Ann. New York Acad. Sci.* **582**, 233-251.

Kiehart, D. P., Montague, R. A., Rickoll, W. L., Foard, D. and Thomas, G. H. (1994). High-resolution microscopic methods for the analysis of cellular movements in *Drosophila* embryos. In *Methods in Cell Biology*, Vol. 44 (ed. L. S. B. Goldstein and E. A. Fyrerg), pp. 507-532. San Diego: Academic Press.

Kiehart, D. P., Galbraith, C. G., Edwards, K. A., Rickoll, W. L. and Montague, R. A. (2000). Multiple forces contribute to cell sheet morphogenesis for dorsal closure in *Drosophila*. *J. Cell Biol.* **149**, 471-490.

Kilchherr, F., Baumgartner, S., Bopp, D., Frei, E. and Noll, M. (1986). Isolation of the *paired* gene of *Drosophila* melanogaster and its spatial expression during early embryogenesis. *Nature* **321**, 493-499.

Kockel, L., Zeitlinger, J., Staszeski, L. M., Mlodzik, M. and Bohmann, D. (1997). Jun in *Drosophila* development: redundant and nonredundant functions and regulation by two MAPK signal transduction pathways. *Genes Dev.* **11**, 1748-1758.

Letsou, A., Arora, K., Wrana, J., Simin, K., Twombly, V., Jamal, J., Staehling-Hampton, K., Hoffman, M., Gelbart, W., Massague, J. et al. (1995). *Drosophila* Dpp signaling is mediated by the *punt* gene product: a dual ligand-binding type II receptor of the TGFβ receptor family. *Cell* **80**, 899-908.

Lu, Y. and Settleman, J. (1999). The *Drosophila* Pkn protein kinase is a Rho/Rac effector target required for dorsal closure during embryogenesis. *Genes Dev.* **13**, 1168-1180.

Magie, C. R., Meyer, M. R., Gorsuch, M. S. and Parkhurst, S. M. (1999). Mutations in the Rho1 small GTPase disrupt morphogenesis and segmentation during early *Drosophila* development. *Development* **126**, 5353-5364.

Martin-Blanco, E., Gampel, A., Ring, J., Virdee, K., Kirov, N., Tolkovsky, A. and Martinez-Arias, A. (1998). *puckered* encodes a phosphatase that mediates a feedback loop regulating JNK activity during dorsal closure in *Drosophila*. *Genes Dev.* **12**, 557-570.

Minden, A., Lin, A., Claret, F.-X., Abo, A. and Karin, M. (1995). Selective activation of the JNK signaling cascade and c-Jun transcriptional activity by the small GTPases Rac and Cdc42. *Cell* **81**, 1147-1157.

Nellen, D., Affolter, M. and Basler, K. (1994). Receptor serine/threonine kinases implicated in the control of *Drosophila* body pattern by decapentaplegic. *Cell* **78**, 225-237.

Nusslein-Volhard, C., Wieschaus, E. and Kluding, H. (1984). Mutations affecting the pattern of the larval cuticle in *Drosophila melanogaster*. I. Zygotic loci on the second chromosome. *R. Arch. Dev. Biol.* **193**, 267-282.

Oda, H., Uemura, T., Harada, Y., Iwai, Y. and Takeichi, M. (1994). A *Drosophila* homolog of cadherin associated with Armadillo and essential for embryonic cell-cell adhesion. *Dev. Biol.* **165**, 716-726.

Ohshiro, T., Yagami, T., Zhang, C. and Matsuzaki, F. (2000). Role of cortical tumour-suppressor proteins in asymmetric division of *Drosophila* neuroblast. *Nature* **408**, 593-596.

Peng, C. Y., Manning, L., Albertson, R. and Doe, C. Q. (2000). The tumour-suppressor genes *lgl* and *dlg* regulate basal protein targeting in *Drosophila* neuroblasts. *Nature* **408**, 596-600.

Penton, A., Chen, Y., Staehling-Hampton, K., Wrana, J., Attisano, L., Szidonya, J., Cassill, A., Massague, J. and Hoffman, M. (1994). Identification of two bone morphogenetic protein type I receptors in *Drosophila* and evidence that Brk25D is a decapentaplegic receptor. *Cell* **78**, 239-250.

Ricos, M. G., Harden, N., Sem, K. P., Lim, L. and Chia, W. (1999). Dcdc42 acts in TGFβ signaling during *Drosophila* morphogenesis: distinct roles for the Drac1/JNK and Dcdc42/TGF-B cascades in cytoskeletal regulation. *J. Cell Sci.* **112**, 1225-1235.

Riesgo-Escovar, J. R. and Hafen, E. (1997). *Drosophila* Jun kinase regulates expression of *decapentaplegic* via the ETS-domain protein Aop and the AP-1 transcription factor DJun during dorsal closure. *Genes Dev.* **11**, 1717-1727.

Riesgo-Escovar, J., Jenni, M., Fritz, A. and Hafen, E. (1996). The *Drosophila* Jun-N-terminal kinase is required for cell morphogenesis but not for DJun-dependent cell fate specification in the eye. *Genes Dev.* **10**, 2759-2768.

Ring, J. M. and Martinez Arias, A. (1993). *puckered*, a gene involved in position-specific cell differentiation in the dorsal epidermis of the *Drosophila* larva. *Development* **Suppl.**, 251-259.

Ruberte, E., Marty, T., Nellen, D., Affolter, M. and Basler, K. (1995). An absolute requirement for both the type II and type I receptors, *punt* and *thick veins*, for Dpp signaling in vivo. *Cell* **80**, 889-897.

Sluss, H., Han, Z., Barrett, T., Goberdhan, D., Wilson, C., Davis, R. and Ip, Y. (1996). A JNK signal transduction pathway that mediates morphogenesis and an immune response in *Drosophila*. *Genes Dev.* **10**, 2745-2758.

Staehling-Hampton, K., Laughon, A. and Hoffmann, F. (1995). A *Drosophila* protein related to the human zinc finger transcription factor PRDII/MBPI/HIV-EP1 is required for *dpp* signaling. *Development* **121**, 3393-3403.

Strutt, D. I., Weber, U. and Mlodzik, M. (1997). The role of RhoA in tissue polarity and Frizzled signaling. *Nature* **387**, 292-295.

Takaishi, K., Sasaki, T., Kotani, H., Nishioka, H. and Takai, Y. (1997). Regulation of cell-cell adhesion by Rac and Rho small G proteins in MDCK cells. *J. Cell Biol.* **139**, 1047-1059.

Tepass, U., Gruszynski-DeFeo, E., Haag, T. A., Omatyar, L., Török, T. and Hartenstein, V. (1996). *shotgun* encodes *Drosophila* E-cadherin and is preferentially required during cell rearrangement in the neuroectoderm and other morphologically active epithelia. *Genes Dev.* **10**, 672-685.

Thomas, G. H. and Kiehart, D. P. (1994). B_{heavy}-spectrin has a restricted tissue and subcellular distribution during *Drosophila* embryogenesis. *Development* **120**, 2039-2050.

Uemura, T., Oda, H., Kraut, R., Hayashi, S., Kataoka, Y. and Takeichi, M. (1996). Zygotic *Drosophila* E-cadherin expression is required for processes of dynamic epithelial cell rearrangement in the *Drosophila* embryo. *Genes Dev.* **10**, 659-671.

Winter, C. G., Wang, B., Ballew, A., Royou, A., Karess, R., Axelrod, J. D. and Luo, L. (2001). *Drosophila* Rho-associated kinase (*Drok*) links Frizzled-mediated planar cell polarity signaling to the actin cytoskeleton. *Cell* **105**, 81-91.

Young, P. E., Richman, A. M., Ketchum, A. S. and Kiehart, D. P. (1993). Morphogenesis in *Drosophila* requires nonmuscle myosin heavy chain function. *Genes Dev.* **7**, 29-41.

Zhao, D. B., Cote, S., Jahnig, F., Haller, J. and Jaeckle, H. (1988). *zipper* encodes a putative integral membrane protein required for normal axon patterning during *Drosophila* neurogenesis. *EMBO J.* **7**, 1115-1119.

Zhong, C., Kinch, M. S. and Burridge, K. (1997). Rho-stimulated contractility contributes to the fibroblastic phenotype of Ras-transformed epithelial cells. *Mol. Biol. Cell* **8**, 2329-2344.

Zhou, L., Schnitzler, A., Agapite, J., Schwartz, L. M., Steller, H. and Nambu, J. R. (1997). Cooperative functions of the *reaper* and *head involution defective* genes in the programmed cell death of *Drosophila* central nervous system midline cells. *Proc. Natl. Acad. Sci. USA* **94**, 5131-5136.